Available online at www.sciencedirect.com
ScienceDirect
Scripta Materialia 64 (2011) 753–756
Scripta MATERIALIA
www.elsevier.com/locate/scriptamat

Indentation size effect in bulk metallic glass

Jae-il Jang,[a,*] Byung-Gil Yoo,[a] Yong-Jae Kim,[a] Jun-Hak Oh,[a] In-Chul Choi[a] and Hongbin Bei[b,*]

[a] *Division of Materials Science and Engineering, Hanyang University, Seoul 133-791, Republic of Korea*
[b] *Materials Science and Technology Division, Oak Ridge National Laboratory, Oak Ridge, TN 37831-6115, USA*

Received 9 December 2010; revised 25 December 2010; accepted 26 December 2010
Available online 31 December 2010

We systematically explored the indentation size effect (ISE), which is not expected to occur in non-crystalline materials due to the absence of dislocations and strain hardening, in bulk metallic glass (BMG). A series of nanoindentation experiments with different indenters result in somewhat surprising observations that show that ISE clearly does exist in BMG and can even be described by the ISE model for crystalline materials. The results are discussed in terms of possible mechanisms responsible for the ISE in BMG.

Keywords: Nanoindentation; Bulk amorphous materials; Hardness; Size effect

With the rapid advances in small-scale mechanical testing techniques over the past two decades, fundamental knowledge about the size effects on the strength and plasticity of crystalline materials has widened remarkably. A representative example of such size effects is the so-called indentation size effect (ISE), which is manifested as an increase in hardness H with decreasing impression size A, indentation depth h or peak load P_{max} (see the recent review [1]). While the ISE was often observed during nanoindentation experiments made with a geometrically self-similar pyramidal indenter (such as the commonly used Berkovich and Vickers indenters), the size-dependency of the hardness H (defined as P_{max}/A) could not be explained by continuum plasticity concepts for which there is no inherent material length scale and thus the H should be independent of the A. To analyze this intriguing phenomenon, early works on the ISE mostly adopted strain gradient plasticity theory (that is, geometrically necessary dislocations (GNDs) would nucleate for accommodating plastic strain gradients in bending or indentation, and thus would increase the strength) and proposed possible relationship between the GNDs and the ISE [1]. The most popular mechanism-based ISE model was established by Nix and Gao [2], who considered the density of GNDs (generated by a sharp indenter) together with a Taylor's dislocation strengthening model. In the Nix–Gao model [2], the relation between the indentation hardness (H) and the indentation depth (h) can be simply described as

$$\frac{H}{H_0} = \sqrt{1 + \frac{h^*}{h}} \tag{1}$$

where h^* is a characteristic length and H_0 is the macroscopic indentation hardness (when h is much greater than h^*). The h^* is given as

$$h^* = \frac{81}{2} b\alpha^2 \cot^2\theta \cdot \left(\frac{G}{H_0}\right)^2 \tag{2}$$

where b is the Burgers vector, α is a geometric constant, θ is the half-cone angle and G is the shear modulus. Since the linear relation between $(H)^2$ and $(1/h)$ in Eq. (1) successfully predicted the experimental indentation hardness data for many crystalline materials, the Nix–Gao model has been applied extensively [1].

Since the Nix–Gao model is based on dislocation strengthening, one may imagine that the ISE does not occur in materials which have a non-crystalline (amorphous) structure or show no strain hardening. An interesting example of such materials is bulk metallic glasses (BMGs), which have recently attracted much interest from both the scientific and technological viewpoints. BMGs do not contain crystalline defects such as dislocations, so dislocation-mediated plasticity does not occur in these materials. Instead, they exhibit a unique form of plastic deformation: at ambient temperature, plastic strain is highly localized into very narrow "shear bands" within which are a densely population of collective atomic rearrangements called shear transformation zones (STZs; these are the

* Corresponding authors. E-mail addresses: jijang@hanyang.ac.kr; beih@ornl.gov

1359-6462/$ - see front matter © 2010 Acta Materialia Inc. Published by Elsevier Ltd. All rights reserved.
doi:10.1016/j.scriptamat.2010.12.036

fundamental carriers of plasticity in metallic glasses) [3]. Due to this shear-band-mediated plasticity, the size-dependent hardness cannot be expected in BMGs, however, some researchers have reported ISE-like behavior in Zr-, Pd-, and Fe-based BMGs [4–11].

While only a limited number of reports have been published concerning the possibility of the ISE phenomenon in BMGs, many more studies have been devoted to a different type of size effect on the strength of BMGs, i.e. the sample size effect (SSE) on strength from uniaxial compression/tension tests of nano-/micropillar samples [12–25]. However, there is no consensus on the SSE of BMGs; some researchers have shown that "smaller is stronger" [12,13,23–25], whereas others have reported the opposite trend [14,19]. It has been also proposed that the strength of BMG is actually size-independent [15–18,20–22]. It is noteworthy that there are clear differences in the mechanical environment between nanoindentation and uniaxial nano-/micropillar tests, which may lead to the different mechanisms for the ISE and SSE. First, unlike pillar tests, the plasticity (and fracture) in the highly stressed volume beneath the indenter is constrained by the surrounding materials, and thus catastrophic failure does not occur during indentation. Secondly, and more importantly, complex three-dimensional stress/strains and strain gradients are developed in the sample during indentation whereas the uniaxial pillar sample experiences almost no strain gradient. Therefore, unlike the ISE, the SSE cannot be explained by the strain gradients. Even for crystalline materials in which the ISE and SSE usually follow the same "smaller is stronger" trend, different mechanisms have been developed, i.e. the strain gradients model for the ISE and the dislocation starvation model for the SSE, as reviewed in Ref. [26].

In this work, we systematically analyzed the possibility of ISE in a Zr-based BMG through nanoindentations with a series of three-sided pyramidal indenters having different indenter angles from 35.3° to 70°. The purpose of this letter is to report our somewhat surprising observations that clear ISE does indeed exist in the BMG and can be described by the Nix–Gao rule originally suggested for crystalline materials [2].

The bulk metallic glass examined in this work is a Zr-based BMG, $Zr_{52.5}Cu_{17.9}Ni_{14.6}Al_{10}Ti_5$ (referred to as Vit 105), which was produced in the form of a rod having a diameter and length of about 7 and 70 mm, respectively. The non-crystalline structure of the sample was confirmed by the absence of a crystalline peak in the X-ray diffraction pattern (shown elsewhere [27]). Nanoindentation experiments were performed using a Nanoindenter-XP instrument (MTS Corp., Oak Ridge, TN) at various loads in the range from 5 to 500 mN. Four different triangular pyramidal indenters having centerline-to-face angles, ψ, of 35.3° (cube-corner), 50°, 65.3° (Berkovich) and 70° were employed. The accuracy of the angle was reported by the manufacturer to be within ±0.15°. In all the nanoindentation experiments the tests were performed at a constant indentation strain rate of 0.05 s^{-1} and the thermal drift was maintained below 0.05 nm s^{-1}. All the hardness impressions were imaged using a JSM-6330F field-emission scanning electron microscope (SEM; JEOL Ltd., Tokyo, Japan) to measure the actual area of the contact. The topological feature of the indented surface was also identified by an XE-100 atomic force microscope (AFM; Park Systems, Suwon, Korea).

Representative examples of load–displacement (P–h) curves recorded during nanoindentation at various peak loads (P_{max}) up to 500 mN (except for the sharpest case of 35.3°, in which the highest peak load was set to be 200 mN to avoid the tip breaking at high loads) are provided in Supplementary material (see Figure S1). It is evident that, for a given P_{max}, a sharper indenter (i.e. an indenter having a smaller angle) produced a larger peak-load displacement (h_{max}), implying that a sharper indenter induces greater stresses and strains in the material due to the larger volume of displaced material [28–30].

The beauty of nanoindentation technique is that one can estimate the hardness and effective modulus by only P–h curve analysis, without observation of the indentation impression. The most popular way to perform this analysis is the Oliver–Pharr method [31], which was also used to calculate the BMG hardness in most of the previous works reporting the ISE-like behavior of BMGs [4–11].

In the present work, however, we did not adopt the Oliver–Pharr method for two reasons. First, in BMG samples, severe material pile-up is usually observed around the indentation impression. Such pile-up is not taken into consideration in the Oliver–Pharr method, and it can thus induce an overestimation of the calculated hardness. In this regard, it is interesting to note that recently Charleux et al. [32] reported a more pronounced pile-up at smaller displacements in nanoindentations of Vitroly-1 BMG. If this holds true, the amount of pile-up-induced overestimation may be greater at smaller depth, which could result in the ISE-like trend and even asks the question: is the reported ISE-like behavior an artifact related to miscalculations of the hardness? To clarify this issue, the pile-up amount here was evaluated through AFM analysis (see Fig. 1). It was revealed that, while the ratio of the pile-up height ($h_{pile\text{-}up}$) to the maximum displacement (h_{max}), $h_{pile\text{-}up}/h_{max}$, for the Berkovich indenter (centerline-to-face angle $\psi = 65.3°$) increased with reducing peak load (which is in good agreement with Charleux et al.'s results [32]), the opposite trend was observed for the cube-corner indenter ($\psi = 35.3°$). This inconsistency in trends (possibly due to the increased influence of friction for a sharper indenter) may make the analysis of the hardness variation more complex.

Second, in the Oliver–Pharr method [31], the correlation constant β (which relates stiffness S to area A in the Oliver–Pharr method) is important for determining the area function and thus the hardness. However, the proper β is known only for the commonly used Berkovich indenter (as a constant of 1.034 [31]), and the dependency of the β value on the indenter angle is still unclear [28], which

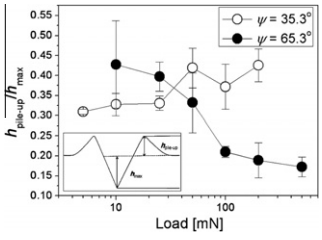

Figure 1. Variation in pile-up amount as a function of indentation load.

may lead to miscalculations of the hardness data for other indenters used in this study and thus make it difficult to directly compare the hardness data from different indenters.

To overcome these difficulties and obtain accurate hardness values, we measured the impression size A directly from a large number of SEM images (see Fig. S2 in Supplementary Material), then obtained the hardness according to the relation $H = 4P/(3\sqrt{3}a^2)$, where a is the averaged length measured from the center of the triangular impression to the corner. The variation in hardness is summarized as a function of displacement in Figure 2a, where, interestingly, the ISE is clearly observed for all the indenters used. It should be noted that, although the hardness for a sharper indenter appears to be the greater at a given displacement h, the hardness measured with different indenters cannot be directly compared for a fixed h. This is simply because, at a given P_{max}, the h becomes deeper for a sharper indenter.

Because all used indenters yielded the ISE, we have attempted to examine whether the ISE can be described according to Eq. (1), i.e. the Nix–Gao model. Figure 2b shows the plots of the square of hardness (H^2) obtained from SEM images against the reciprocal of the indentation depth ($1/h$). A high linearity between H^2 and $1/h$ is seen for all used indenters. One of the interesting predictions of the Nix–Gao model is that there is a strong dependence of the hardness behavior on the indenter angle. According to

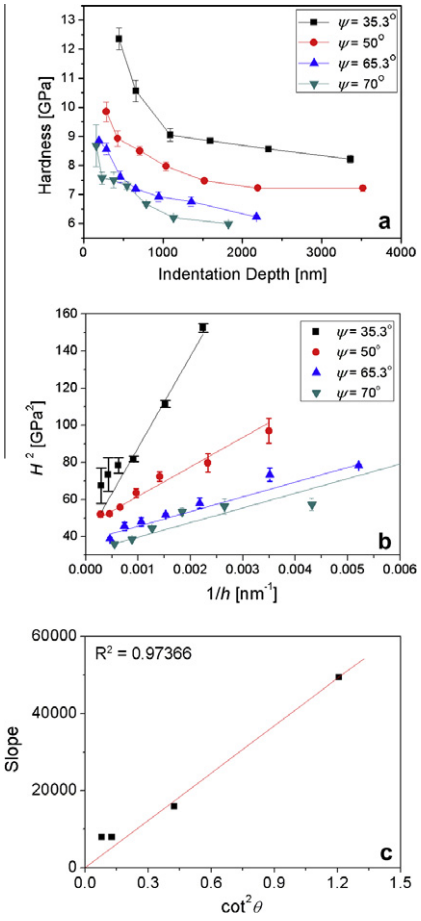

Figure 2. Analysis of hardness data according to the Nix–Gao model: plots of (a) hardness H vs. penetration depth; (b) H^2 vs. $1/h$; and (c) slope of linear relations in (a) vs. $\cot^2\theta$.

Eqs. (1) and (2), it is apparent that the slope of the linear relation between H^2 and $1/h$ should rely on $\cot^2\theta$, which varies by an order of magnitude depending on one's choice of tip. To relate the conical indentation used for Eqs. (1) and (2) to triangular pyramidal indentation in this work, it is useful to make the normal assumption that similar behavior is obtained when the angle of the cone gives the same area-to-depth ratio as the pyramid, which gives the half-cone angle θ as $\theta = \tan^{-1}(\sqrt{\frac{3\sqrt{3}}{\pi}}\tan\psi)$, where ψ is the centerline-to-face angle. Thus, ψ values of 35.3°, 50°, 65.3° and 70° correspond to θ values of 42.3°, 56.9°, 70.3° and 74.2°, respectively.

In Figure 2c, the slopes of the straight lines in Figure 2b are plotted against $\cot^2\theta$. Somewhat surprisingly, the plot has very high linearity, implying that the Nix–Gao model indeed agrees very well with the indentation data for a wide range of indenter angles.

Two important questions are why does the ISE exist for non-crystalline materials and how can the ISE be fitted by the Nix–Gao model? While the detailed mechanisms are still far from completely understood, the suggestions made in the limited publications reporting the ISE-like behavior [4–11] can be roughly categorized into three groups (to our best knowledge). The first group [4,7] comprises the models constructed in a way very analogous to that used in the Nix–Gao model; the mechanisms proposed by Lam and Chong [4] and more recently by Yang et al. [7] also adopted the perspective of strain gradient plasticity, and the only difference between their models and the Nix–Gao model is that they used the concept of non-crystalline flow defects instead of dislocations. The basic assumption in their theories is that the plasticity induced by a strain gradient should be accommodated by "geometrically necessary" flow defects (either shear clusters [4] or excess free volumes [7]), which can be given as

$$H \propto \sqrt{V_S + V_G} \tag{3}$$

where V_S and V_G are the densities of the statistically stored defects and the geometrically necessary defects. Therefore, the increased density of the defects at shallow indentation depth is mainly responsible for the ISE in a BMG, as the increase in the GNDs is in the Nix–Gao model. However, this scenario may not be reasonable, simply because the increase in the glass defects (e.g. excess free volume [3]) would induce softening rather than hardening in the metallic glass [27,33,34].

The second group of the suggestions [5,8] is focused on the strain softening [27,33,34] and on the dependence of hardness on the strain rate imposed during the indentation. Van Steenberge et al. [8] argued that, for a given strain rate, the continuous accumulation of excess free volume during deformation can cause strain softening at large penetration depth and this softening is the source of the ISE. They then established a relationship between the hardness and the strain rate based on the classical metallic glass flow equations developed by Spaepen [35] and Argon [36]:

$$H(\approx 3\sqrt{3}\tau) \propto \sinh^{-1}(\alpha\dot{\gamma}/c_f) \tag{4}$$

where τ is the shear stress, α is a constant, $\dot{\gamma}$ is the shear strain rate and c_f is the concentration of flow defects. Based on this relation, they argued that, as the indenta-

tion strain rate, $d\varepsilon_i/dt = h^{-1}(dh/dt)$ [8,29], diminishes during indentation testing under a constant loading rate (dP/dt), the high indentation strain rate at shallow depth can induce an increase in hardness [8]. However, this possibility could be excluded in the present study because all indentation experiments were performed under a constant strain rate instead of a constant loading rate (see Fig. S3 in Supplementary Material). Another shortcoming in this argument is that the strain softening equation does not take into consideration the geometrical self-similarity of a sharp indenter. From a classical contact mechanics perspective, the stress (or hardness) and the strain underneath a sharp indenter should not vary during indenter penetration. Therefore, in their result, the hardness change is an experimentally obtained result (or output) rather than controllable input parameter. Thus, this hypothesis can be largely viewed as empirical rather than analytical.

The third group considers the influences of the surface effect (including residual stress and friction) [6,9–11] to be the main cause of the possible ISE in BMG. However, since they did not account for the strain gradient induced by a self-similar indenter, there is no way to explain the angle effect that is very clear in this study.

Collectively, we conclude that the ISE phenomenon observed in the present work cannot be explained by any of the existing models and should be interpreted in a different way. A new possibility we suggest here is that the occurrence of STZs [3] might be controlled by the indentation size or the volume of the indentation-induced elastic/plastic deformation. For shallow indentations, the highly stressed volume beneath the indenter is probably too small to have a sufficient population of STZs (which can evolve into the highly active shear bands, which, in turn, are able to accommodate the plastic deformation) and thus the shear bands are forced to operate at a particular location, whereas deep indentations produce a large volume of deformation and thus higher activities of STZs and shear bands. In this regard, a higher hardness might be observed for low-load indentations because the glass is demanded to shear in particular locations. Additionally, this hypothesis can conceivably explain the angle effect on hardness (i.e. the seemingly higher hardness for a sharper indenter shown in Fig. 2a and b) in a qualitative manner. For a given h (not for a given P_{max}), a sharper indenter having smaller θ (or ψ) produces a smaller contact radius a and thus a smaller highly-stressed or plastic zone (which is often considered to be proportional to a^3; for example, $2\pi a^3/3$ in the Nix–Gao model). Therefore, at a given h, lower activities of STZs and higher hardness may be expected for a sharper indenter, which is in agreement with the trend in the present work.

This research was supported by the Basic Science Research Program through the National Research Foundation of Korea (NRF) funded by the Ministry of Education, Science and Technology (No. 2010-0025526). The research at ORNL (H.B.) was sponsored by the US Department of Energy, Office of Basic Energy Sciences, Materials Sciences and Engineering Division. We thank Prof. W.D. Nix and the anonymous reviewer for valuable comments.

Supplementary data associated with this article can be found, in the online version, at doi:10.1016/j.scriptamat.2010.12.036.

[1] G.M. Pharr, E.G. Herbert, Y. Gao, Annu. Rev. Mater. Res. 40 (2010) 271.
[2] W.D. Nix, H. Gao, J. Mech. Phys. Solids 46 (1998) 411.
[3] C.A. Schuh, T.C. Hufnagel, U. Ramamurty, Acta Mater. 55 (2007) 4067.
[4] D.C.C. Lam, A.C.M. Chong, Mater. Sci. Eng. A 318 (2001) 313.
[5] A. Concustell, J. Sort, G. Alcalá, S. Mato, A. Gebert, J. Eckert, M.D. Baró, J. Mater. Res. 20 (2005) 2719.
[6] I. Manika, J. Maniks, Acta Mater. 54 (2006) 2049.
[7] F. Yang, K. Geng, P.K. Liaw, G. Fan, H. Choo, Acta Mater. 55 (2007) 321.
[8] N. Van Steenberge, J. Sort, A. Concustell, J. Das, S. Scudino, S. Surinach, J. Eckert, M.D. Baró, Scripta Mater. 56 (2007) 605.
[9] N. Li, K.C. Chan, L. Liu, J. Phys. D: Appl. Phys. 41 (2008) 155415.
[10] N. Li, L. Liu, K.C. Chan, J. Mater. Res. 24 (2009) 1693.
[11] N. Li, L. Liu, K.C. Chan, Q. Chen, J. Pan, Intermetallics 17 (2009) 227.
[12] C.J. Lee, J.C. Huang, T.G. Nieh, Appl. Phys. Lett. 91 (2007) 161913.
[13] Q. Zheng, S. Cheng, J.H. Strader, E. Ma, J. Xu, Scripta Mater. 56 (2007) 161.
[14] Y.J. Huang, J. Shen, J.F. Sun, Appl. Phys. Lett. 90 (2007) 081919.
[15] C.A. Volkert, A. Donahue, F. Spaepen, J. Appl. Phys. 103 (2008) 083539.
[16] B.E. Schuster, Q. Wei, T.C. Hufnagel, K.T. Ramesh, Acta Mater. 56 (2008) 5091.
[17] A. Dubach, R. Raghavan, J.F. Löffler, J. Michler, U. Ramamurty, Scripta Mater. 60 (2009) 567.
[18] X.L. Wu, Y.Z. Guo, Q. Wei, W.H. Wang, Acta Mater. 57 (2009) 3562.
[19] Y. Wu, H.X. Li, G.L. Chen, X.D. Hui, B.Y. Wang, Z.P. Lu, Scripta Mater. 61 (2009) 564.
[20] C.Q. Chen, Y.T. Pei, J.T.H.M. De Hosson, Phil. Mag. Lett. 89 (2009) 633.
[21] H. Bei, Z.P. Lu, S. Shim, G. Chen, E.P. George, Metall. Mater. Trans. A 41 (2010) 1735.
[22] C.Q. Chen, Y.T. Pei, J.T.H.M. De Hosson, Acta Mater. 58 (2010) 189.
[23] C.J. Lee, Y.H. Lai, J.C. Huang, X.H. Du, L. Wang, T.G. Nieh, Scripta Mater. 63 (2010) 105.
[24] D. Jang, J.R. Greer, Nature Mater. 9 (2010) 215.
[25] A. Bharathula, S.W. Lee, W.J. Wright, K.M. Flores, Acta Mater. 58 (2010) 5789.
[26] W.D. Nix, J.R. Greer, G. Feng, E.T. Lilleodden, Thin Solid Films 515 (2007) 3152.
[27] B.G. Yoo, K.W. Park, J.C. Lee, U. Ramamurty, J.I. Jang, J. Mater. Res. 24 (2009) 1405.
[28] J.H. Strader, S. Shim, H. Bei, W.C. Oliver, G.M. Pharr, Philos. Mag. 86 (2006) 5285.
[29] J.I. Jang, B.G. Yoo, J.Y. Kim, Appl. Phys. Lett. 90 (2007) 211906.
[30] J.I. Jang, G.M. Pharr, Acta Mater. 56 (2008) 4458.
[31] W.C. Oliver, G.M. Pharr, J. Mater. Res. 7 (1992) 1564.
[32] L. Charleux, S. Gravier, M. Verdier, M. Fivel, J.J. Blandin, Mater. Sci. Eng. A 483–484 (2008) 652.
[33] H. Bei, S. Xie, E.P. George, Phys. Rev. Lett. 96 (2006) 105503.
[34] B.G. Yoo, Y.J. Kim, J.H. Oh, U. Ramamurty, J.I. Jang, Scripta Mater. 61 (2009) 951.
[35] F. Spaepen, Acta Metall. 25 (1977) 407.
[36] A.S. Argon, Acta Metall. 27 (1979) 47.